

OPEN ACCESS

Effect of X-ray Line Spectra Profile Fitting with Pearson VII, Pseudo-Voigt and Generalized Fermi Functions on Asphalt Binder Aromaticity and Crystallite Parameters

To cite this article: K Gebresellasie *et al* 2012 *J. Phys.: Conf. Ser.* **397** 012069

View the [article online](#) for updates and enhancements.

You may also like

- [Estimation of soil water content using electromagnetic induction sensors under different land uses](#)
Clinton Mensah, Yeukai Katanda, Mano Krishnapillai et al.
- [Equivariant Hopf bifurcation in a ring of identical cells with delayed coupling](#)
Sue Ann Campbell, Yuan Yuan and Sharene D Bungay
- [A new method for speckle reduction in Synthetic Aperture Radar \(SAR\) images using optimal window size](#)
S Mahdavi, B Salehi, C Moloney et al.

ECS
The
Electrochemical
Society
Advancing solid state &
electrochemical science & technology

DISCOVER
how sustainability
intersects with
electrochemistry & solid
state science research

Effect of X-ray Line Spectra Profile Fitting with Pearson VII, Pseudo-Voigt and Generalized Fermi Functions on Asphalt Binder Aromaticity and Crystallite Parameters

K Gebresellasi¹, J Shirokoff² and J C Lewis¹

¹Department of Physics and Physical Oceanography, Memorial University of Newfoundland, St. John's, Newfoundland, A1B 3X7, Canada

²Faculty of Engineering and Applied Science, Memorial University of Newfoundland, St. John's, Newfoundland, A1B 3X5, Canada

E-mail: john.lewis@mun.ca

Abstract. X-ray line spectra profile fitting using Pearson VII, pseudo-Voigt and generalized Fermi functions was performed on asphalt binders prior to the calculation of aromaticity and crystallite size parameters. The effects of these functions on the results are presented and discussed in terms of the peak profile fit parameters, the uncertainties in calculated values that can arise owing to peak shape, peak features in the pattern and crystallite size according to the asphalt models (Yen, modified Yen or Yen-Mullins) and theories. Interpretation of these results is important in terms of evaluating the performance of asphalt binders widely used in the application of transportation systems (roads, highways, airports).

Keywords: asphaltene; x-ray scattering; profile fitting

PACS: 81.05.-t; 81.40.-z; 81.70.-q.

1. Introduction

Asphalt binder is a black colored, sticky, viscous liquid (semi-solid) of varying chemical composition dependant on feedstock such as crude oil, bituminous coal, and natural sources. Asphalt binder production is mostly derived from petroleum refining (distillation) of crude oils. The three major components that are usually found in asphalt binders consist of asphaltenes, resins and oils (aromatic hydrocarbons) [1]. The molecular structure of asphalt binder is an important feature since it affects the physical and aging (oxidation) properties of asphalt as well as how the molecules may interact with each other and with additional components such as crushed stone often used in the construction of roads, highways, and airport runways, for example.

Asphaltenes are molecules that consist of carbon, hydrogen, nitrogen, oxygen, sulfur, and trace amounts of metals such as nickel and vanadium. The molecular weight (MW) of asphaltenes is on average about MW=750 Da with FWHM of 500 to 1000 Da [1,2]. They have been studied by techniques originally developed for colloids including x-ray diffraction (XRD) in order to quantify asphaltene molecular length scales [1-8]. Initial research by Yen et al created the Yen model in order to explain aromatic stacking and the mechanism from molecular to cluster states in asphaltenes [3-4]. Additional research led to further refinement of the Yen model and creation of the modified Yen model or Mullins-Yen model as a consequence of explaining the transformation of asphaltene molecules into asphaltene nanoaggregates and clusters of nanoaggregates [2,6-8]. The purpose of this

paper is to focus on some of the recent spectral line shape data derived from XRD profile fits using three different mathematical functions on calculating aromaticity and crystallite parameters, and subsequently to link these data to asphalt science models.

2. Experimental

The asphalt binder samples (T2 to T7) were obtained from Northern Ontario, and Alberta, Canada. The asphalt grades and location (town, city) in Canada can be found elsewhere [9]. Thin films deposits of sample (>1 mm) were prepared by coating onto glass slide holders followed by heating to 150°C for 10 minutes in a drying oven and air cooled at ambient (25°C).

Standard XRD methods previously developed by Warren, Franklin and Diamond and have been used to study petroleum asphaltenes with improvements in instrumentation and computer software [10]. The overall research program involved collecting XRD spectra that were obtained immediately after preparation and also after aging for 1 week and 6 weeks at low-temperature (-10°C) [9-10]. In this study various samples after 1 week of aging were measured by XRD and analyzed. The x-ray diffraction spectral scans were obtained by Rigaku D/Max-2200V-PC using monochromatic Cu K α radiation at 40 kV and 40 mA. The scan range was 5° to 110° 2 θ at a scan rate of 0.001° 2 θ per second and detector count time of 5 seconds/step. The XRD instrument employed a divergence slit of 0.5° and receiving slit of 0.3mm.

The XRD spectra were then peak searched using a parabolic filter (99 raw data points, screened out K α -2 peaks, peak location summit, threshold sigma 3.0, intensity cutoff 0.1%, range to find background 1.0, points to average background 7) over the angular range of 5° to 110°. The full width at half-maximum (FWHM) and profile fits were obtained by using either Pearson VII and pseudo-Voigt function (fixed background, exponent = 1.5 and Lorentzian = 0.5) over the ranges 5° to 35° 2 θ and 60° to 110° 2 θ on the XRD line spectra of interest. The XRD spectra were also modeled in Mathematica © software using a generalized Fermi function (GF) which was previously described in the literature [11].

3. Results and discussion

The spectral line shape of an XRD pattern from sample T3 is shown in figure 1 left, (full spectrum top, profile fit bottom), with several peaks: an overlapping peak in the low-angle range (0° to 30° 2 θ) that contains both the γ -band (left side) and the (002)-graphene band (right side). The (002)-graphene band represents the spacing between the layers of a condensed aromatic system, while the γ -band defines the packing distance of saturated structures such as the aliphatic chains or condensed saturated rings. The two broad peaks which appear in the middle (30° to 60° 2 θ) and high (60° to 110° 2 θ) angle portions of the spectra are indexed as the (10) reflection and (11) reflection, analogous to the second (100) and third (110) most close-packed planes in face-centered-cubic (fcc) metal systems, that correspond to the first and second nearest neighbors in ring structured compounds. The method for obtaining the aromaticity f_a and crystallite parameters (aromatic sheet diameter L_a , cluster size L_c , interlayer distance between aromatic sheets d_M , interchain distance d_γ , and number of sheets per cluster M_e) were all obtained from the x-ray diffraction spectra according to standard methods [3-4,9-10].

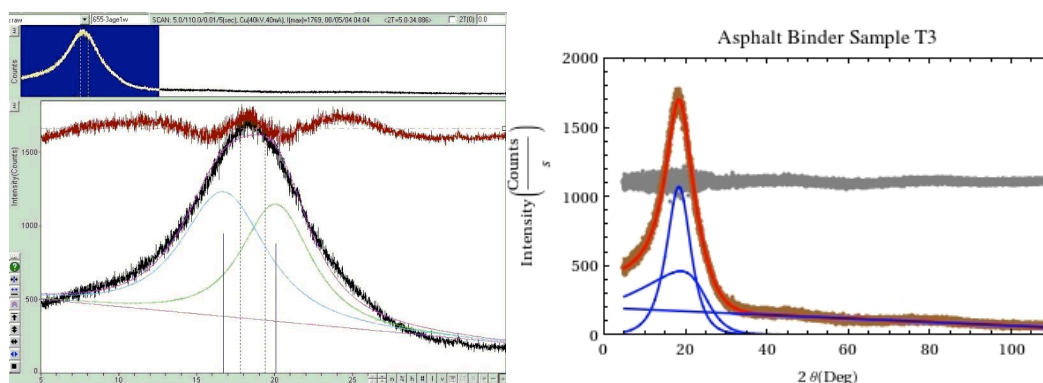


Figure 1. Left: X-ray diffraction spectra (top) and Pearson VII profile fit spectra and analysis curves (bottom) for sample T3; Right: GF-Mathematica © profile fit spectra for sample T3.

As previously described [9-10] and used in the GF results, the aromaticity f_a was determined by calculating the areas A of the resolved peaks for the γ and the (002)-graphene using the following formula:

$$f_a = C_A/C = C_A/(C_A + C_S) = A(\text{graphene})/A(\text{graphene}) + A(\gamma) \quad (1)$$

where C_S , C_A and C are the number of saturated, aromatic and total carbon atoms per structural unit, respectively [9-10]. Since the equation used for the calculation of the f_a is based only on the stack-cluster aromatic carbon to the (002)-graphene peak and is not due to all the aromatic carbons of asphaltene, f_a does not represent a true aromaticity of the molecules but rather an estimate. A second issue arises from the use of the profile fitting program for Pearson VII versus pseudo-Voigt functions where the Pearson VII function favors larger γ -peak areas, $A(\gamma)$, relative to (002)-graphene peak areas, $A(\text{graphene})$. This second issue consequently calculates a higher aromaticity value when using the pseudo-Voigt function compared to the Pearson VII function calculations as seen in Table 1. A third issue arises when comparing calculations from the three functions as it concerns profile fitting the two major peaks in the low-angle spectrum (γ -peak and (002)-graphene peak) in the presence of additional peaks (i.e. paraffin peaks). Under these conditions equation (1) becomes questionable unless it is replaced with more variables to account for three or more peaks over the low-angle spectral range and validated by experimental results. Moreover, the fundamental diffraction method used in this case to calculate aromaticity should be questioned since it assumes that the γ -peak comes from all aliphatic carbons present (ie. paraffins and naphthenes) but in fact the γ -peak arises primarily from paraffins [10-12]. The generalized Fermi function results are poorly correlated to pseudo-Voigt and Pearson VII in the case of samples T6 and T7 presumably due to a lack of symmetry in the XRD data. The XRD data profiles in the low-angle spectral range of 5° to 10° 2θ varies from sample to sample and appears to be influenced by the symmetry of the two major peaks (γ -peak and (002)-graphene) affecting the sensitivity of the profile fitting process. Also, x-ray scattering is influenced by variations in asphaltene size and number of molecules (~ 1.5 nm), nanoaggregates (~ 2 nm), and clusters (~ 5 nm) as reported in the modified Yen model [6]. Smaller asphaltene sizes and larger numbers of asphaltene will lead to XRD line (peak) broadening effects. Since an increased volume fraction of small sized nanomaterial is known to alter stress-strain behavior, and strengthen solids (i.e. metals due to delocalized electrons) this becomes an important feature with respect to asphalt interfaces and interphase boundaries that will play a greater role in structure-property behavior of asphalt binder materials.

The interlayer distance between the aromatic sheets d_M , was calculated using Bragg's Law and the maximum of the (002) graphene band according to

$$d_M = \lambda / (2 \sin \theta) \quad (2)$$

where d_M is the interlayer distance, λ is the wavelength of the Cu K_α radiation and θ is Bragg's angle. The results in Table 1 indicate about the same d_M values using the pseudo-Voigt function however in

the past asphaltene binder studies the values were higher for pseudo-Voigt due to consistently smaller measured 2θ values when compared to data generated using Pearson VII [10].

The distance between the saturated portions (aliphatic chains, condensed saturated rings) molecules or interchain layer distance is given by the relationship:

$$d_\gamma = 5\lambda/(8 \sin\theta) \quad (3)$$

The interchain layer distance d_γ results in Table 1 trended towards higher values using the pseudo-Voigt function due to consistently smaller measured 2θ values when compared to the data generated by the Pearson VII and generalized Fermi. This trend in measuring crystallite parameters in equations (2) and (3) is related to the measuring functions (Pearson VII, pseudo-Voigt, generalized Fermi) in a low-angle spectral range that appears shape-related since the spectrum in this range is unsymmetrical.

Table 1. Aromaticity and crystallite parameters for asphalt binders calculated using Pearson VII (P), pseudo-Voigt (V), and generalized Fermi (GF) functions on line profile fits of the XRD spectra for various samples after 1 week of low-temperature aging.

	f_a			d_M (Å)			d_γ (Å)			L_a (Å)			L_c (Å)			M_e		
	P	V	GF	P	V	GF	P	V	GF	P	V	GF	P	V	GF	P	V	GF
T2	0.53	0.66	0.58	4.5	4.5	4.7	6.9	7.3	6.0	3.7	3.7	3.8	5.2	4.4	5.2	2.2	2.0	2.1
T3	0.53	0.60	0.52	4.5	4.5	4.2	7.0	7.2	6.0	3.3	3.3	3.3	5.3	4.6	4.7	2.2	2.0	2.1
T4	0.55	0.69	0.55	4.5	4.6	4.7	7.0	7.4	6.3	3.2	3.2	3.3	5.2	4.4	4.7	2.2	2.0	2.0
T5	0.49	0.57	0.59	4.5	4.5	4.8	6.9	7.1	5.7	3.4	3.4	3.3	6.2	5.4	5.7	2.4	2.2	2.2
T6	0.65	0.73	0.08	4.6	4.6	7.1	7.6	8.0	6.0	3.1	3.1	3.3	4.4	3.9	4.3	2.0	1.8	1.6
T7	0.52	0.53	0.28	4.5	4.5	5.2	6.9	6.9	5.9	3.3	3.3	3.1	5.9	6.3	5.2	2.3	2.4	1.9

The average diameter of the aromatic sheets is calculated from the following formula incorporating the Scherrer equation for measuring mean crystallite size:

$$L_a = 1.84\lambda/(\omega \cos\theta) = 0.92/B_{1/2} \quad (4)$$

where $B_{1/2}$ is the FWHM using the (11) band and ω is the bandwidth. The results calculated for average diameter of the aromatic sheets are about the same in value for all three profile fitting functions.

The average height of the stack of aromatic sheets perpendicular to the sheet plane was calculated using the following formula:

$$L_c = 0.9\omega \cos\theta = 0.45/B_{1/2} \quad (5)$$

where $B_{1/2}$ is the FWHM using the (002)-graphene band. The results calculated for L_c in Table 1 are mostly larger for Pearson VII values compared to pseudo-Voigt fitted profiles. These calculations are the result of smaller (002)-graphene band FWHM measured values using Pearson VII in all samples but one (sample T7) which has additional paraffin (wax) peaks in the low-angle spectrum and wax is detrimental to asphalt performance [9].

The number of aromatic sheets in a stacked cluster, M_e , was calculated from the values of L_c and d_M according to the following relationship:

$$M_e = (L_c/d_M + 1) \quad (6)$$

It is not surprising that the results for the number of aromatic sheets in a stacked cluster, M_e , are generally higher in all samples (except T7) analyzed using Pearson VII compared to pseudo-Voigt, since these results are were influenced more by the change in values of L_c than that found in d_M .

When comparing our data to those obtained by small angle neutron scattering (SANS) and small angle x-ray scattering (SAXS) we find our values to be slightly lower for L_c higher for d_M and lower for M_e [2]. The main reason for this discrepancy requires accounting for the solvated solution asphaltene samples used by the authors of [2] compared to the dry asphaltenes used in our studies and by Yen et al. in order to understand the more extended stacking of nanoaggregates in dry asphaltene samples, especially as reported for Yen's samples.

4. Conclusions

Aromaticity and average crystallite parameters in asphalt binders can be calculated using XRD data and profile fits with various functions (Pearson VII, pseudo-Voigt, and generalized Fermi). With these parameters it is possible to consider a hypothetical average molecular basis for evaluating the material on a macro-to-nano scale that will aid in the physical and chemical understanding of complex materials such as asphaltene as it relates to line broadening, stress-strain, interphase-interfaces, and applications in transportation systems (roads, highways, airports). However, the pseudo-Voigt profile has weak theoretical support in this context, and the Pearson VII, which has the benefit that it can interpolate smoothly between Gaussian and Lorentzian shapes (centrosymmetric), is nonetheless entirely empirical [10]. Unfortunately, the generalized Fermi function results are less well correlated to Pearson VII and pseudo-Voigt since they appear to be more influenced by asymmetry in the XRD spectra. The results build on the modified Yen model and asphaltene theories where spectral features are correlated with the micro-to-nano-crystallinity in asphaltenes.

References

- [1] Mullins O C et al. Eds 2007 *Asphaltenes, Heavy Oils and Petroleomics*, Springer, New York
- [2] Eyssautier J, Levitz P, Espinat P et al. 2011 *J. Phys. Chem B* **115** 6827-37
- [3] Yen T F 1992 *Fuel Sci. Technol. Int.* **10** 723-33 (1992).
- [4] Yen T F, Erdman J G and Pollack S S 1961 *Anal. Chem.* **33** 1587-94
- [5] Tanaka R, Sato E, Hunt J E et al. 2004 *Energy Fuels* **18** 1118-25
- [6] Mullins O C 2010 *Energy Fuels* **24** 2179-207
- [7] Mullins O C et al. 2010 *Offshore Technology Conf*, **OTC 20464** 1
- [8] Goual L, Sedghi M, Zeng H et al. 2011 *Fuel* **90** 2480-90
- [9] Hesp S A M, Iliuta S and Shirokoff J 2007 *Energy Fuels* **21** 1112-21
- [10] Shirokoff J, Lewis J C 2010 *20th Int. Conf. Spectral Line Shapes*, CP1290 AIP 274
- [11] Aldea N, Tiusan C V, Barz B 2004 *J. Optoelectronics Adv. Materials* **6** 225-35
- [12] Siddiqui M N, Ali M F and Shirokoff J 2002 *Fuel* **81** 51-8